Neutronic Design and Assessment of SSCR Core Compared with a Conventional PWR

Youngrok Lee, Hyun Chul Lee*
School of Mechanical Engineering, Pusan National University, 2, Busandaehak-ro 63beon-gil, Geumjeong-gu, Busan, 46241, Republic of Korea
**Corresponding author: hyunchul.lee@pusan.ac.kr*

***Keywords :** H_2O–D_2O moderator, SSCR, PWR, fuel utilization, cycle length*

1. Introduction

Unlike a conventional pressurized water reactor (PWR), which controls its excess reactivity mainly through neutron absorption in soluble boron, a spectral shift control reactor (SSCR) controls reactivity by hardening the neutron spectrum, exploiting the lower slowing-down power of heavy water (D_2O) relative to that of light water (H_2O) [1]. In an SSCR, a high D_2O fraction is maintained at the beginning of cycle (BOC) to compensate for the large excess reactivity. In the experimental work [2], reactivity was subsequently controlled through stepwise H_2O addition combined with temperature feedback.

For the SSCR concept to achieve economic competitiveness within a conventional PWR framework, the core should be designed to preserve practical PWR design characteristics, such as sufficiently high power density and a compact core size, while exploiting the improved neutron economy provided by D_2O. Accordingly, the SSCR design should leverage established PWR technologies and design features to minimize additional R&D requirements and development costs. In the present study, several lattice candidates were evaluated while maintaining the volumetric power density and core volume of a conventional PWR. Simplified core models based on the selected lattice configurations are subsequently developed and compared in terms of their neutronic performance. All neutronic calculations were carried out using the Monte Carlo neutron transport code MCS [3]. In addition, a scoping-level thermal-hydraulic analysis was performed using the LWR subchannel code COBRA-EN [4]. Although COBRA-EN does not fully account for the thermophysical properties of H_2O–D_2O coolant mixtures, it was employed for a preliminary comparative assessment of MDNBR and fuel temperature among the candidate geometries.

2. Methods and Results

To characterize the neutronic effects of H_2O–D_2O mixtures discussed below, pin-cell and fuel-assembly calculations were performed using two-dimensional models. UO_2 fuel enriched to 4.95 wt% ^{235}U was used throughout the analysis. The D_2O content is defined as the volume fraction of D_2O in the moderator mixture. A lattice with a larger moderator volume is hereafter referred to as a *wetter* geometry, whereas one with a smaller moderator volume is referred to as a *drier* geometry. The lattice geometry of a conventional large PWR is used as the reference geometry throughout this study.

2.1 Lattice design

In a conventional PWR, excessively high excess reactivity at BOC requires a high soluble boron concentration, which may shift the lattice into the over-moderated regime. Fig. 1 shows the pin-cell k_∞ as a function of the moderator-to-heavy-metal volume ratio (M/HM), which was varied by changing the pin pitch. Results are presented for D_2O volume fractions ranging from 0% to 100% and soluble boron concentrations of 1500 and 3000 ppm. At 1500 ppm, the reference geometry lies close to the optimum moderation condition, whereas at 3000 ppm—which provides a reactivity worth comparable to that achieved with a D_2O fraction of 50–75% in the reference geometry—the lattice shifts into the over-moderated regime. For H_2O–D_2O mixtures, a lower D_2O fraction corresponds to a higher hydrogen content. Because hydrogen has a substantially larger neutron absorption cross section than deuterium, the optimum moderation point shifts toward a drier lattice condition as the H_2O fraction increases. The slope of k_∞ with respect to M/HM further indicates that, for M/HM < 4.0, where the lattice remains under-moderated even with 0% D_2O, increasing the D_2O fraction results in a more negative MTC. These results suggest that the feasible SSCR design space can be extended into the under-moderated regime (M/HM < 4.0), where lattice configurations may simultaneously provide higher excess reactivity, maintain a negative MTC, and improve fuel utilization [5].

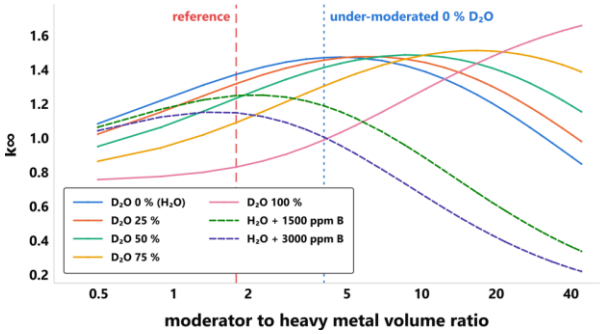


Fig. 1. M/HM vs. k_∞ for various moderator conditions (pin pitch variation).

In the lattice design, pin-cell geometries were considered that maintain the volumetric power density

and core volume of a conventional PWR while avoiding degradation of the thermal-hydraulic safety margins. Three lattice configurations, consisting of one reference lattice and two wetter candidate lattices, were evaluated. The candidate pitches were selected so that 17 × 17 and 18 × 18 fuel assemblies could be constructed with approximately the same assembly width as the conventional 16 × 16 PWR assembly. Within these geometric constraints, wetter lattices were considered provided that their thermal-hydraulic safety margins were not degraded relative to the reference. The thermal-hydraulic performance was assessed in terms of the MDNBR and maximum fuel centerline temperature, while each lattice was additionally required to remain under-moderated at 0% D_2O.

The thermal-hydraulic analysis was performed using the LWR subchannel code COBRA-EN at a volumetric power density representative of the APR1400 [6]. Accordingly, the pin-cell volume determines the average linear heat rate. For each geometry, the coolant mass flow rate was adjusted to maintain the same inlet and outlet coolant temperatures under the average-power condition. A three-dimensional single hot-channel model was then used for the thermal-hydraulic assessment. Hot-channel conditions derived from the APR1400 core calculations were imposed, including a 3% engineering uncertainty factor, a radial pin peaking factor of 1.55, and a cosine-shaped axial power distribution, resulting in a total peaking factor of 2.35 [6]. The gap conductance was fixed at 10,000 W/m²·K, and the W-3 correlation was used for the DNBR evaluation.

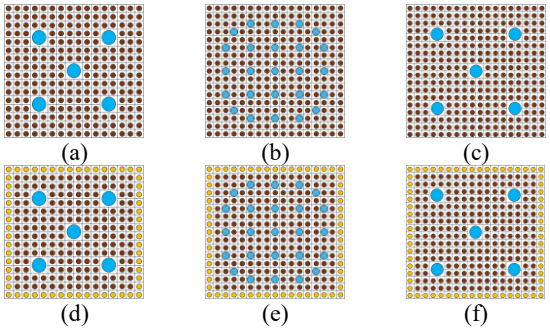
Table I summarizes the principal design parameters and analysis results for the three pin-cell configurations. The reference configuration corresponds to the lattice geometry employed in a large conventional PWR, whereas Candidates 1 and 2 are wetter lattices designed to maintain the same volumetric power density while preserving thermal-hydraulic margins comparable to those of the reference lattice. Compared with the reference, both candidates employ smaller pellet radii and reduced pin pitches while maintaining nearly the same hydraulic diameter. The three-dimensional hot-channel analysis gives an MDNBR of 2.67 and a maximum fuel centerline temperature of 1990 K for the reference lattice, and the corresponding results for the candidate lattices are also listed in Table I. The neutronic depletion calculations were performed using two-dimensional pin-cell models with 4.95 wt% enriched fuel. A 4% neutron leakage was assumed, corresponding to an end-of-cycle criticality criterion of k_∞=1.04. Owing to their higher M/HM and improved neutron economy, their relative discharge burnups, normalized to that of the reference lattice, are approximately 7% and 12% higher than the reference, respectively. However, because the wetter lattices contain less fuel at the same volumetric power density, they operate at higher specific power. Consequently, their relative cycle lengths are slightly shorter at the same fuel enrichment despite the higher discharge burnup.

Table I: Pin-cell parameters and results.

Parameter	Reference	Cand. 1	Cand. 2
Pellet radius (cm)	0.4096	0.3696	0.3316
Pin pitch (cm)	1.285	1.210	1.142
Height (cm)	381	381	381
M/HM	1.79	2.02	2.34
Hydraulic dia. (cm)	1.263	1.273	1.294
Inlet temp. (K)	563.75	563.75	563.75
Outlet temp. (K)	598.15	598.15	598.15
Mass flux (kg/m²·s)	3635.8	3493.5	3350.2
MDNBR (W-3)	2.67	2.70	2.68
Max. fuel temp. (K)	1990	1818	1678
Burnup (rel.)	1.0	1.07	1.12
Cycle length (rel.)	1.0	0.98	0.93

2.2 Assembly design

Fig. 2 shows the three fuel-assembly configurations constructed from the pin-cell geometries examined above, including the adopted fuel enrichment zoning. Compared with the 16 × 16 reference assembly used in current large PWRs, Candidates 1 and 2 achieve nearly the same assembly width when configured as 17 × 17 and 18 × 18 arrays, respectively. The candidate assemblies also have slightly larger fuel-pin-to-water-hole ratios than the reference assembly. Because the SSCR maintains a negative MTC and controls excess reactivity throughout the cycle through the gradual addition of H_2O, assembly designs without burnable absorbers were considered. Fuel enrichment zoning was instead employed to mitigate local power peaking at the core level, mainly at the interfaces between assemblies of different enrichment. Fig. 3 shows the pin power distributions at D_2O fractions corresponding to the reactivity control required at the beginning of Cycle 1 of a large PWR. Table II summarizes the corresponding pin power peaking factors obtained from two-dimensional assembly calculations for three moderator conditions: pure H_2O, soluble-boron-loaded H_2O, and H_2O–D_2O mixtures. For each lattice, the soluble boron concentration and D_2O fraction were selected to provide comparable reactivity control worth. The H_2O–D_2O mixtures exhibit lower local power peaking around the water holes than the H_2O-based moderator cases. This behavior is attributed to the lower local moderating power and longer neutron migration length of the H_2O–D_2O mixture, which result in stronger spatial coupling over neighboring cells and a smoother pin power distribution.



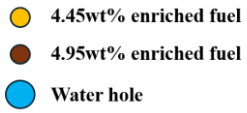


Fig. 2. Fuel assembly configurations: (a)–(c) uniform 4.95 wt% enrichment and (d)–(f) enrichment-zoned layouts for the reference 16 × 16, Candidate 1 17 × 17, and Candidate 2 18 × 18 assemblies.

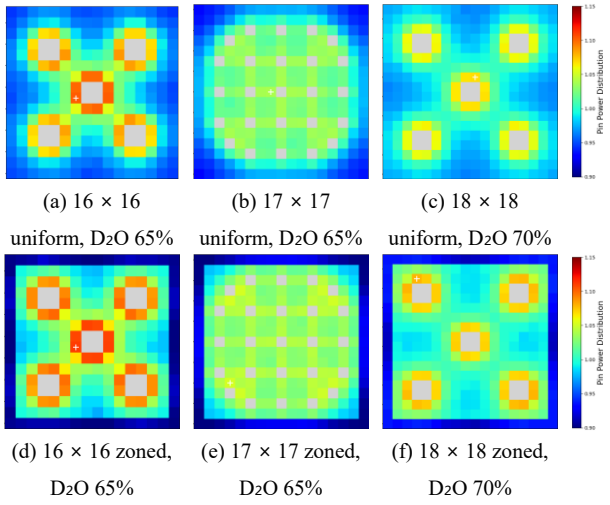


Fig. 3. Assembly pin power distributions with H_2O–D_2O moderator mixtures.

Table II: Assembly pin power peaking factors (U = uniform enrichment, Z = enrichment-zoned; soluble boron 3000/3000/2500 ppm and D_2O 65/65/70% for the Reference, Cand. 1, and Cand. 2 lattices).

Case	Reference		Cand. 1		Cand. 2	
	U	Z	U	Z	U	Z
H_2O	1.15	1.15	1.06	1.07	1.11	1.12
Boron	1.15	1.13	1.06	1.07	1.10	1.11
D_2O	1.08	1.11	1.04	1.05	1.07	1.08

2.3 Core design

For the core-level calculations, Cycle 1 of the OPR1000 was modeled as the reference case, with the SSCR cores evaluated at the same core-average enrichment of approximately 2.35 wt% [7]. Axial reflectors, each 30 cm thick, were modeled above and below the active core. To reduce computational cost, a core model with homogenized structural materials was employed.

The core depletion calculations were performed without thermal feedback. For the reference PWR, the Cycle 1 burnable absorber configuration of OPR1000 was modeled [7], and the critical boron concentration (CBC) was determined at each depletion step. In contrast, the SSCR cores employed only the enrichment-zoned assemblies described above, without burnable absorbers, and a single loading pattern was constructed using these assemblies. Table III summarizes the assembly types used in each core, and Fig. 4 shows the corresponding loading pattern. The SSCR loading pattern was designed to reproduce the overall radial power distribution of the low-leakage PWR reference core while maintaining the radial power peaking factor, F_r, below 1.55.

Table III: Assembly types and fuel enrichments used in the SSCR loading pattern (values separated by a slash denote the inner/peripheral enrichment zones).

Assembly type	Fuel enrichment (wt% ^{235}U)		
	16 × 16	17 × 17	18 × 18
A0	1.25	1.25	1.25
B0	2.25	2.25	2.25
C0	2.75	2.75	2.75
C1	2.75/2.25	2.75/2.25	2.75/2.25
D0	3.25	3.25	3.25
D1	3.25/2.75	3.25/2.75	3.25/2.75

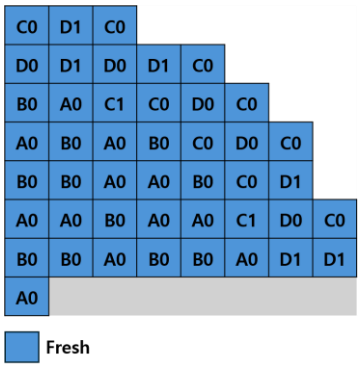


Fig. 4. Assembly loading pattern using the assembly types defined in Table III.

The PWR depletion calculation was continued until the critical boron concentration decreased to 10 ppm, whereas the SSCR depletion calculations were terminated when the critical D_2O fraction reached approximately 2–3%. Fig. 5 compares the critical boron concentration as a function of burnup for the PWR with the critical D_2O fraction for the SSCR cores. The corresponding discharge burnups and cycle lengths are summarized in Table IV. Relative to the reference PWR core, the 16 × 16, 17 × 17, and 18 × 18 SSCR cores achieve increases in discharge burnup of approximately 2.7, 3.7, and 3.9 GWd/MTU, respectively, with corresponding cycle-length extensions of approximately 73.6, 56.0, and 27.2 days. These improvements are achieved despite the lower total fuel inventories of the SSCR cores.

For the 18 × 18 core, the discharge burnup and cycle-length extension were smaller than expected from the pin-cell depletion analysis, primarily because of the relatively low fuel enrichment employed in the Cycle 1 loading. Further evaluation under equilibrium-cycle conditions, where higher-enrichment reload fuel is employed, is therefore required to assess the full potential of the 18 × 18 configuration.

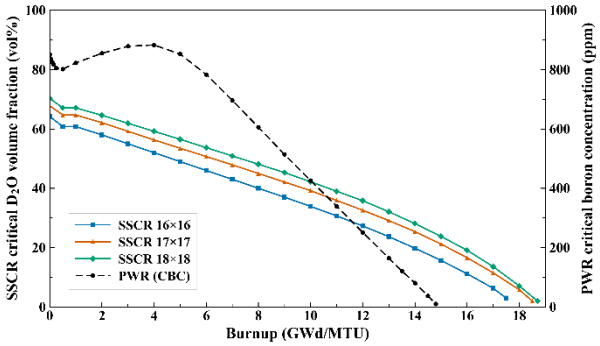


Fig. 5. Critical D_2O volume fraction of the SSCR cores (left axis) and critical boron concentration of the reference PWR (right axis) as functions of burnup.

Table IV: Discharge burnup (GWd/MTU) and cycle length (EFPD) of the reference PWR and SSCR cores.

Parameter	PWR	SSCR		
		16 × 16	17 × 17	18 × 18
Burnup	14.8	17.5	18.5	18.7
Cycle length	400.5	474.1	456.5	427.7

3. Conclusions

This study assessed the neutronic feasibility of an SSCR core designed within the principal geometric and power-density constraints of a conventional PWR. Pin-cell and assembly analyses showed that the use of an H_2O–D_2O moderator mixture enables wetter lattice designs with improved neutron economy while maintaining an under-moderated condition and a negative MTC. The selected lattice candidates preserved the volumetric power density and approximately the same core size as the reference PWR without degrading the evaluated thermal-hydraulic margins. Core-level local power peaking was mitigated through fuel enrichment zoning instead of burnable absorbers.

Core depletion calculations based on the OPR1000 Cycle 1 configuration showed discharge-burnup increases of approximately 2.7, 3.7, and 3.9 GWd/MTU and cycle-length extensions of approximately 73.6, 56.0, and 27.2 days, respectively, relative to the reference PWR, despite the lower total fuel inventories of the SSCR cores. The relatively limited cycle-length benefit of the 18 × 18 core is attributed in part to the low enrichment of the Cycle 1 loading; therefore, its performance should be further evaluated under equilibrium-cycle conditions employing higher-enrichment reload fuel. Overall, the results demonstrate the potential of H_2O–D_2O spectral-shift control to improve fuel utilization while retaining the power density and core compactness of conventional PWR designs.

Acknowledgments

This work was supported by the National Research Foundation of Korea (NRF) grant funded by the Ministry of Science and ICT (MSIT of Korea) (RS-2024-00436693) and Human Resources Program in Energy Technology of the Korea Institute of Energy Technology Evaluation and Planning (KETEP), which was funded by Ministry of Trade, Industry & Energy (MOTIE of Korea) (No. RS-2024-00398425).

REFERENCES

[1] D. Mars, D. Gans. “Spectral shift control reactor design and economic study,” Office of Technical Services, 1241 (1961).
[2] J. Storrer, S. Rigg. “The Vulcain core power experiment,” Proc. 3rd U.N. Conference on the Peaceful Uses of Atomic Energy, 1 (1964).
[3] H. Lee, et al. “MCS–A Monte Carlo particle transport code for large-scale power reactor analysis,” Annals of Nuclear Energy, 139, 107276 (2020).
[4] D. Basile, et al. “COBRA-EN: an upgraded version of the COBRA-3C/MIT code for thermal-hydraulic transient analysis of light water reactor fuel assemblies and cores,” In: Report No. 1010/1, ENEL SpA, Milan, Italy (1987).
[5] B.A. Lindley, G.T. Parks. “The Spectral Shift Control Reactor as an option for much improved uranium utilisation in single-batch SMRs,” Nuclear Engineering and Design, 309, pp. 75-83 (2016).
[6] APR1400-K-X-FS-14002-NP, Revision 3, “APR1400 Design Control Document Tier 2,” KHNP, December 2018.
[7] The Nuclear Design Report for Yonggwang Nuclear Power Plant Unit 1 Cycle 1, KAERI/TR-542/95, Korea Atomic Energy Research Institute, 1995.